J. Opt. A: Pure Appl. Opt. **9** (2007) 431–434 doi:10.1088/1464-4258/9/5/001

Artefacts in polarization modulation scanning near-field optical microscopes

R Micheletto[1], **M Allegrini**[2] **and Yoichi Kawakami**[1]

[1] Department of Electronic Science, Graduate School of Engineering, Kyoto University, Nishigyo-ku, Katsura, 615-8510 Kyoto, Japan
[2] Department of Physics, University of Pisa, Largo Pontecorvo 3, 56127 Pisa, Italy

E-mail: ruggero.micheletto@optomater.kuee.kyoto-u.ac.jp

Received 11 May 2006, accepted for publication 14 March 2007
Published 3 April 2007
Online at stacks.iop.org/JOptA/9/431

Abstract
The objective of this study is to model a polarization modulation scanning near-field optical microscope set-up (PM-SNOM) and demonstrate how the influence of real instruments as photodetector and lock-in produces a coupling between signals that generates intrinsic artefacts on experimental data. A simple polar coordinates mathematical framework has been used to derive an analytical expression of the relevant signals. A simulation of typical experimental cases is presented and contrast artefacts more than 100% are demonstrated. This study is effective for an accurate analysis of PM-SNOM tests and it is of general use for the discussion of artefacts in polarization modulation systems.

Keywords: SNOM, polarizator, birefringence, dichroism, optical fibres

(Some figures in this article are in colour only in the electronic version)

A scanning near-field optical microscope (SNOM) is a device used to investigate the optical properties of a sample at a resolution higher than conventional optical microscopy [1, 2]. Near-field interactions are highly dependent on the polarization properties of the sample. However, SNOM systems are more often used to study local transmittivity (reflectivity or refractivity depending on configuration [3]), local fluorescence, local spectra or other confined information. Sample polarization properties are often neglected or considered not position-dependent. In other words, they are assumed to have a constant influence throughout the SNOM map; however, in some SNOM tests the main target is the study of the local polarization characteristics of a sample [4–7]. Here we want to discuss the polarization modulation SNOM (PM-SNOM) where the light is polarization modulated and detected locally by the use of a lock-in amplifier tuned to the frequency of modulation. We will develop a rigorous model of a PM-SNOM system; using a simple polar framework we will explain the influence of real instrumentation on the signals by giving an analytical expression for each of them. We will demonstrate that there is unexpected intrinsic cross-talk between local transmittivity and local polarization properties giving rise to perceptible artefacts in the PM-SNOM maps.

We consider the PM-SNOM system shown in figure 1: light emitted from point xy on the sample is filtered by a rotating polaroid, and the optical signal is then detected by a phototube, then its output is fed to a lock-in amplifier. The relevant data are three maps that we will call P^{xy}, R^{xy} and Ph^{xy} (the xy superscript represents the spatial coordinate on the sample), proportional to the optical signal at the photon counter and to the signal at the lock-in in modulation and phase, respectively.

There are well known specialized formalisms to describe the polarization of the light through optical elements [8–10]. However, since our discussion will include the effect of real instruments on signals, Fourier transformation and integration will be necessary. To simplify and make the treatment easily comprehensible we developed a polar coordinate framework where the light is considered incoherent, achromatic and formally always linearly polarized. It is represented by the two elements of a polar vector $(\phi,\ \rho)$, where ϕ is the angular phase and ρ the intensity. To consider the general case we need to represent also not-polarized light. We achieve this by defining a vector of intensity ρ and of undefined angle $\langle\phi\rangle$. This definition has been chosen because it is the most natural for numerical treatment and it is compatible with the actual physical nature of not-polarized light, that it is a combination

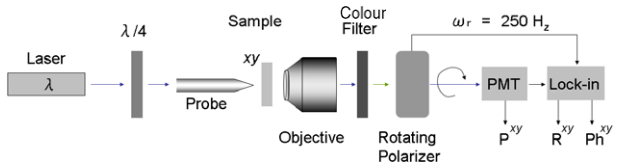

Figure 1. The PM-SNOM set-up modelled. The probe illuminates the sample and induces a confined optical emission from point xy. The resulting light emission is then polarization modulated using a linear polarizer mounted on a motor revolving at ω_r. The signal at the photodetector (a PMT in this example) is fed to the lock-in device tuned to the modulation frequency. Signals P^{xy}, R^{xy} and Ph^{xy} from PMT and from lock-in are collected and mapped simultaneously. Colour filter is not relevant to the model; it is placed only to represent a typical photoluminescence experiment.

Table 1. The elements along the optical line are represented by these operators. The rotating polarizer operator P_{ol} forces its angle $\theta = \omega_r t$, thus converting the light into linear polarization. With regard to the intensities it simply applies the Malus law to a polarized vector and does not affect a not-polarized one. The operator representing the photodetector P_{ct} integrates the amplitude using the detector time constant τ_{pc}. Finally the lock-in is represented by the operator Li that calculates the Fourier component of the signal locked to ω_r. See text for details.

Rotating polarizer	$\begin{cases} P_{ol}\left[\begin{pmatrix}\phi\\ \rho\end{pmatrix}\right]_{\theta=\omega_r t} = \begin{pmatrix}\omega_r t\\ \rho\cos^2(\phi-\omega_r t)\end{pmatrix} \\ P_{ol}\left[\begin{pmatrix}\langle\delta\rangle\\ \rho\end{pmatrix}\right]_{\theta=\omega_r t} = \begin{pmatrix}\omega_r t\\ \rho\end{pmatrix} \end{cases}$
Photodetector	$P_{ct}\left[\begin{pmatrix}\phi\\ \rho(t)\end{pmatrix}\right]_{\tau_{pc}} = \int_t^{t+\tau_{pc}} \rho(t')\,\mathrm{d}t'$
Lock-in	$Li[\rho(t)]_{\tau_{li}=2\pi/\omega_r} = 2\mathrm{i}\int_0^{\tau_{li}} \rho(t')\mathrm{e}^{-\mathrm{i}\omega_r t}\,\mathrm{d}t'$

of random polarization states. Moreover, the formalism must take in account the local nature of the PM-SNOM experiment, so every position-dependent parameter will be assigned the apex xy.

Labelling with a and b the not-polarized and polarized intensities we obtain this expression:

$$\begin{pmatrix}\phi^{xy}\\ \rho^{xy}\end{pmatrix} = \begin{pmatrix}\langle\delta\rangle\\ k^{xy}\rho_a^{xy}\end{pmatrix} + \begin{pmatrix}\alpha^{xy}\\ k^{xy}\rho_b^{xy}\end{pmatrix} \tag{1}$$

representing the light coming off the sample from point xy. The top element of each vector is the polarization angle, that is a random value $\langle\delta\rangle$ for not-polarized light and α^{xy} in the case of polarization.

The factor k^{xy} is a position-dependent coefficient that takes into account that the sample is illuminated point by point on a bidimensional area and the degree of illumination is not *a priori* the same in each point. In other words, the matrix k^{xy} is representing a pure transmittivity phenomena on the sample. This illustrates the typical artefact we might observe in an actual experiment. For example, when we monitor photoluminescence and measure an upsurge of the emission at xy, we cannot be sure whether it is due to an increased concentration of fluorescent material, or whether there has been a simple boost of the local transmittivity, or else whether it was a combination of both. Writing the expression as in (1) explicitly takes this fact into account.

This optical field is filtered by a polaroid rotating with speed ω_r. Using the operators in table 1, we have:

$$\begin{aligned}\begin{pmatrix}\phi^{xy}\\ \rho^{xy}\end{pmatrix}_{P_{ol}} &= P_{ol}\left[\begin{pmatrix}\phi^{xy}\\ \rho^{xy}\end{pmatrix}\right] \\ &= \begin{pmatrix}\omega_r t\\ k^{xy}(\rho_a^{xy} + \rho_b^{xy}\cos^2(\alpha^{xy}-\omega_r t))\end{pmatrix}\end{aligned} \tag{2}$$

representing the light just after the rotating polarizer. This is a linearly polarized light with polarization angle rotating with time, and the angular element is $\omega_r t$ where ω_r is the rotation speed and t the time. The amplitude instead is the sum of two parts: the first, ρ_a^{xy}, represents the not-polarized emission (with random phase $\langle\phi\rangle$). This contribution is obviously a constant value independent from the angular position of the polarizer (see table 1). The other represents an emission polarized with an angle α^{xy}, it is $\rho_b^{xy}\cos^2(\alpha^{xy}-\omega_r t)$ according to the Malus law [11].

This field is then fed to the detection device. A photodetector is sensitive only to light modulation, so the $\omega_r t$ component is ignored and the output will be a scalar value. We use the operator P_{ct} of table 1:

$$P^{xy}(t) = k^{xy}\int_t^{t+\tau_{pc}} [\rho_a^{xy} + \rho_b^{xy}\cos^2(\alpha^{xy}-\omega_r t')]\,\mathrm{d}t' \tag{3}$$

where τ_{pc} is the detector integration time. Solving the integral we obtain:

$$P^{xy}(t) = \frac{k^{xy}}{4\omega_r}(r_a + r_b + r_c) \tag{4}$$

where

$$\begin{aligned} r_a &= 2(2\rho_a^{xy} + \rho_b^{xy})\omega_r\tau_{pc} \\ r_b &= \rho_b^{xy}\sin(2\alpha^{xy} - \omega_r t) \\ r_c &= -\rho_b^{xy}\sin(2\alpha^{xy} - 2(\tau_{pc}+t)\omega_r). \end{aligned} \tag{5}$$

$P^{xy}(t)$ is the signal at the photon counter, it is one of the actual experimental data available. The signal is then fed to a lock-in amplifier. This device is tuned to $2\omega_r$ (the factor 2 is necessary because the Malus law doubles the signal frequency). We use the operator L_i in table 1; since the lock-in amplifier is tuned to the frequency of modulation $2\omega_r$ the integral is taken between zero and $\tau_{li} = 2\pi/\omega_r$. Solving the integral and calling the result $C^{xy}(2\omega_r)$ we obtain:

$$C^{xy}(2\omega_r) = 2\mathrm{i}\int_0^{\tau_{li}} P^{xy}(t)\mathrm{e}^{-\mathrm{i}2\omega_r t}\mathrm{d}t \tag{6}$$

$$= k^{xy}\frac{\pi\rho_b^{xy}}{2\omega_r}(\mathrm{e}^{2\mathrm{i}\tau_{pc}\omega_r} - 1)\mathrm{e}^{-2\mathrm{i}\alpha^{xy}}. \tag{7}$$

The lock-in gives two outputs proportional to the module (R) and phase (Ph) of $C^{xy}(2\omega_r)$, thus:

$$R^{xy} = k^{xy}\frac{\pi\rho_b^{xy}}{2\omega_r} \tag{8}$$

$$Ph^{xy} = 2(\alpha^{xy} - \omega_r\tau_{pc}). \tag{9}$$

In conclusion, the expressions for the relevant signals in our PM-SNOM experiment are P^{xy}, R^{xy} and Ph^{xy} as written in (4), (8) and (9).

Noticeably, the signal at the photodetector P^{xy} (4) includes terms of α^{xy}. This means that the signal we measure in this map is not only dependent on the intensity of the light, but also on its polarization properties. Since a PMT

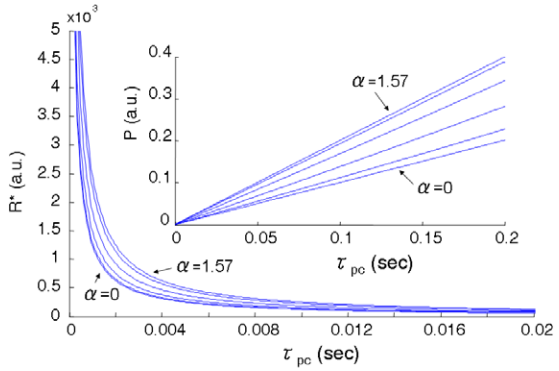

Figure 2. Plot of the signal R_*^{xy} and P^{xy} as a function of τ_{pc} for five values of α ranging from 0 to 1.57 rad. In the inset we show the dependence of P against τ_{pc}. Variation of α induces artefacts of about 100% in both plots. Calculations have been carried out with $t = 0$ s, $\rho_a^{xy} = 1$ au, $\rho_b^{xy} = 1$ au, $\omega_r = 2\pi/10$ rad.

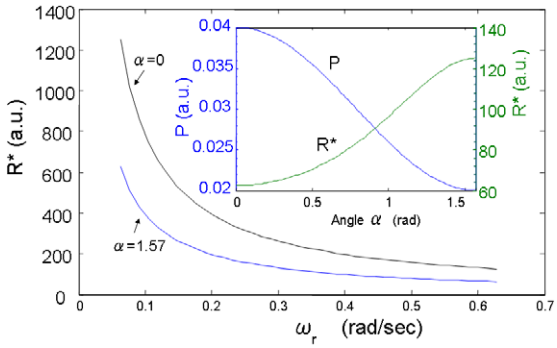

Figure 3. Plot of the signal R_*^{xy} as a function of ω_r for two values of α. In the inset P^{xy} and R_*^{xy} are plotted against the angle. These signals should be independent of α^{xy}. However, we observe differences up to about 100%. Calculations were done with $t = 0$ s, $\rho_a^{xy} = 1$ au, $\rho_b^{xy} = 1$ au, $\omega_r = 2\pi/10$ rad and $\tau_{pc} = 0.02$ s.

or similar detector is not sensitive to polarization, this may look counterintuitive. Nevertheless, any photodetector has its own integration time, and it is this integration process that determines the dependence on α^{xy}. In other terms: in a point xy where light has a polarized component, the signal at the phototube will be oscillating due to filtering through the rotating polaroid. The time phase of this oscillation depends on the angular phase of the light and the result of the integral in (3) depends on it.

To clarify this we plot in figure 2 the integral P as a function of the integration time τ_{pc} for five polarization angles α, ranging from zero to 90° (1.57 rad). The evident discrepancies for different values of α illustrate the concept described above.

The map at the photodetector P^{xy} is affected not only by this instrument-induced polarization-related phenomenon, but also by inherent transmittivity artefacts. Local variations of k^{xy} can induce an increased signal at the photodetector that is not distinguishable from local emissions ρ_a^{xy} or ρ_b^{xy}, as described earlier. One common approach to avoid this artefact is to divide the signal at the lock-in to the photodetector one [5], in our treatment R^{xy}/P^{xy}. According to (4), (5) and (8)

$$R_*^{xy} = \frac{2\pi\rho_b^{xy}}{r_a + r_b + r_c}. \tag{10}$$

This is indeed independent of the transmittivity of the sample. Nevertheless it includes terms containing the local polarization angle α^{xy} and ω_r in the denominator. Figure 3 shows a plot of R_*^{xy} against ω_r for two extreme values of α and indicating the existence of strong contrast artefacts. In the inset the dependence of P^{xy} and R_*^{xy} to the angle is illustrated for typical experimental parameters.

Using (4), (5), (8) and (9) we carried out a simulation to test relevant cases, see figure 4. The simulation generated four 50 × 50 pixel maps. The transmittivity map is set to $k^{xy} = b_o + r$, a constant value $b_o = 5$ plus a random number between 0 and 1 to emulate a background signal. ρ_a^{xy}, ρ_b^{xy} and α^{xy} are as in table 2, where $S = 3$. Five circular domains are defined: these regions are indicated as P_1–P_5. They are defined in order to represent typical emission areas. P_1 is an

Table 2. Description of the emission domains simulated in the calculations. r is a random value between 0 and 1 (r^* between 0 and π), b_o represent background and S the signal.

	k (trasm.)	ρ_a (rand. pol.)	ρ_b (pol.)	α (angle)
P_1	$b_o + r$	$(S + r)/2$	$(S + r)/2$	1.47
P_2	$b_o + r$	r	$S + r$	0.93
P_3	$b_o + r$	r	$S + r$	0.00
P_4	$b_o + r$	$S_n + r$	r	r^*
P_5	$S + b_o + r$	r	$S + r$	0.52

elliptical emission centre, ρ_a^{xy} and ρ_b^{xy} are set to the same value $(S + r)/2$ and the angle of emission set to 1.47 radians. P_2 is a polarized centre at an angle of 0.93 radians. P_3 is another polarized centre, of the same intensity, but different angle (zero radians) and P_4 is a not-polarized emission centre. The region indicated as P_5 is polarized and has the same intensity of P_2 and P_3. It was set to coincide with a high transmittivity area in order to induce a transmittivity artefact.

In the calculations, experimental parameters have been set to $\omega_r = 2\pi f_r$, (polarizer modulation frequency $f_r = 200$ Hz), photon counter integration time is $\tau_{pc} = 2$ ms, and lock-in integration time is set to $\tau_{li} = 2\pi/\omega_r$. Results show that, even if all the signals stand out of the noise of the same amount, emitting regions of different polarization states appear of different intensity in the photodetector map. This is the specific characteristic of (4) and (5) that reveals as a significant crosstalk feature. Also, the values of R map should be related solely to the optical intensity of the polarized emission centres. However, the domain P_5 is conditioned by the higher transmittivity in that region, and appears in the lock-in signal at an increased value. Since this is due to the multiplicative factor k^{xy} in (8), one approach we discussed earlier is to divide the lock-in signal to the photodetector one. Nevertheless, as shown in figure 4(B), the P^{xy} map contains a contrast artefact due to α^{xy} and so putting this map as the denominator will not result in an artefact-free image. The Ph^{xy} map 4(D) is free from contrast artefacts; it represents solely the angular value of the optical emission, independently from its intensity. The angular information is relative and the angle measured is twice the actual polarization angle. Usually PM-SNOM experiments are designed to determine whether

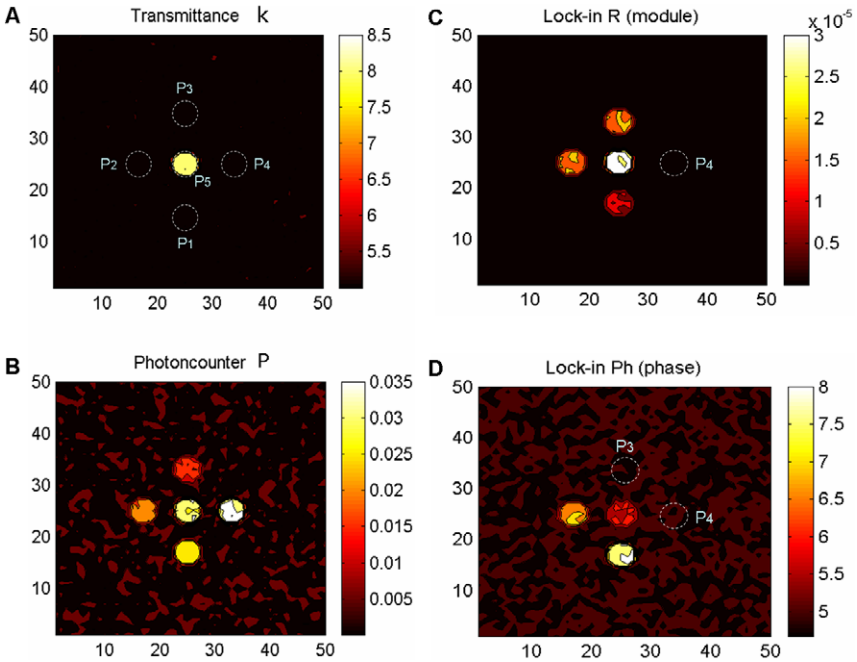

Figure 4. A simulated PM-SNOM experiment is shown. The optical characteristics of the five domains cause different contrast artefacts for different signals shown in the graphs. See table 2 for a description of the five domains and the text for discussion.

the sample has local polarization-altering properties and how intense these properties are at a specific point. However, the Ph^{xy} map does not contain direct information on this, it is simply a map of angles; for example a not-polarized region (P_4) or a polarized one of zero degrees (P_3) will be confused in this map and care must be taken.

We demonstrated rigorously how in a PM-SNOM experiment, the test and the interpretation of the images can be significantly conditioned by the processing device. All maps have to be analysed and compared to reach consistent conclusions. We believe that the analytical expressions obtained in this study and the simulation described may help to avoid erroneous interpretation and support the design of novel and artefact-free polarization modulation systems.

Acknowledgments

We acknowledge with thanks the Kyoto Nanotechnology Cluster for support, Dr Davide Guzzetti of RIMS, Kyoto, Japan and Pietro Gucciardi of CNR, Messina, Italy for their keen observations and comments. This study was carried out within the bilateral project 2A2 of the VII executive program for science and technology cooperation between Japan and Italy.

References

[1] Lewis A and Lieberman K 1991 *Nature* **354** 214–6
[2] Betzig E and Trautman J K 1992 *Science* **257** 189–95
[3] Ohtsu M 1995 *Optoelectron. Devices Technol.* **10** 147–66
[4] Betzig E, Trautman J K, Weiner J S, Harris T D and Wolfe R 1992 *Appl. Opt.* **31** 4563–8
[5] Ambrosio A *et al* 2004 *Nanotechnology* **15** S270–5
[6] Labardi M, Coppede N, Pardi L, Allegrini M, Giordano M, Patane S, Arena A and Cefali E 2003 *Mol. Cryst. Liq. Cryst.* **398** 33–43
[7] Ramoino L, Labardi M, Maghelli N, Pardi L, Allegrini M and Patane S 2002 *Rev. Sci. Instrum.* **73** 2051–6
[8] Shurcliff W A 1966 *Polarized Light* (Cambridge, MA: Harward University Press)
[9] Mueller H 1948 *J. Opt. Soc. Am.* **38** 661–7
[10] Jones R C 1941 *J. Opt. Soc. Am.* **31** 488–93
[11] Hecht E 1975 *Schaum's Outline of Theory and Problems of Optics* (New York: McGraw-Hill)